Systems & Control Transactions

Research Article - Peer Reviewed Conference Proceeding
ESCAPE 35 - European Symposium on Computer Aided Process Engineering
Ghent, Belgium. 6-9 July 2025
Jan F.M. Van Impe, Grégoire Léonard, Satyajeet S. Bhonsale,
Monika E. Polańska, Filip Logist (Eds.)

PSE PRESS

A Novel Objective Reduction Algorithm for Nonlinear Many-Objective Optimization Problems

Hongxuan Wang[a], Andrew Allman[a]*

[a] University of Michigan, Department of Chemical Engineering, Ann Arbor, Michigan, USA
* Corresponding Author: allmanaa@umich.edu

ABSTRACT

Sustainability is increasingly recognized as a critical global issue. Multi-objective optimization is an important approach for sustainable decision-making, but problems with four or more objectives are hard to interpret due to its high dimensions. In our group's previous work, an algorithm capable of systematically reducing objective dimensionality for (mixed integer) linear Problem has been developed. In this work, we will extend the algorithm to tackle nonlinear many-objective problems. An outer approximation-like method is employed to systematically replace nonlinear objectives and constraints. After converting the original nonlinear problem to linear one, previous linear algorithm can be applied to reduce the dimensionality. The benchmark DTLZ5(I, M) problem set is used to evaluate the effectiveness of this approach. Our algorithm demonstrates the ability to identify appropriate objective groupings on benchmark problems of up to 20 objectives when algorithm hyperparameters are appropriately chosen. We also conduct extensive testing on the hyperparameters to determine their optimal settings. Additionally, we analyze the computation time required for different components of the algorithm, ensuring efficiency and practical applicability.

Keywords: Multi-Objective Optimization, Nonlinear Optimization, Outer Approximation.

INTRODUCTION

Optimization is an essential mathematical tool for decision making in the chemical industry, enabling solutions of problems in the design, operation, and control of chemical, pharmaceutical and energy processes. Process system optimization is challenging because models of real chemical systems are often complicated, nonlinear and large scale in terms of variables and equations, incorporating both continuous and discrete decisions. The process systems community has been among the leaders in developing powerful theoretical and algorithmic advances in solving the types of challenging optimization problems encountered in decision making for chemical systems [1, 2]. However, most of this effort has been focused on problems containing a single (usually economic) objective [3]. More recently, the chemical industry has come to the forefront as a sector where adopting sustainable practices is essential. To do so requires considering more than just economic drivers for decision making but also include environmental and social objectives during the optimization of chemical engineering process systems.

When considering problems with multiple objectives, there is in almost all cases competition, or tradeoffs, between the different objectives, which can be visualized in a Pareto frontier which presents a set of solutions corresponding to the best one can do in one objective without degrading the others. Multi-objective optimization is an essential tool to generate Pareto frontiers, particularly for problems of two or three objectives [4]. Scalarization approaches, such as the weighted sum or epsilon constraint approach, can be used to generate a set of single-objective optimization problems which rigorously generate Pareto-optimal solutions. This approach enables chemical engineers to simultaneously consider multiple competing objectives and understand their tradeoffs, enabling informed decision-making. However, many disjoint objectives can be thought of as within the purview of "sustainability", and when dealing with more than four objectives (many-objective problems, or MaOPs), a curse of dimensionality emerges. As the number of objectives increases, the computational effort required to solve these problems using rigorous approaches also grows exponentially.

Moreover, visualizing Pareto frontiers in a four or higher dimension space in order to understand tradeoffs and generate a final decision is challenging. Thus, to our knowledge very few works in the process systems literature today formulate and solve high-dimensional MaOP's for sustainable decision making.

To overcome the challenges of objective dimensionality, systematic objective dimensionality reduction for (mixed-integer) linear MaOPs has been previously proposed by our group [5]. For linear problems, optimal solutions always lie on the boundary of the feasible region when the solution is finite. Thus, it is logical to focus the analysis of objective interactions on constraint surfaces. Gradient vectors of the objective functions are projected onto the constraint surfaces. Inner product of the projected vectors and a weighted sum of the constraint interaction strengths are used to determine the total objective correlation strength. Correlation strength is used as edge weight in an objective correlation graph, which consists of nodes corresponding to the different objectives. Finally, a community detection algorithm is applied to identify groups of objectives. For more details about the objective reduction algorithm, please reference our previous works. It has already been successfully used to analyze the correlating and competing nature of a scheduling MaOPs [6]. However, many real-world optimization challenges, particularly in chemical engineering disciplines like process control and system design, are inherently nonlinear. Nonlinear problems introduce additional complexities due to their behavior and interactions, with solutions often not confined to the edges of the feasible region, as well as the potential for locally optimal solutions when the problem is nonconvex, necessitating a more comprehensive approach. Several methods exist for solving mixed-integer nonlinear problems, such as outer approximation [7], generalized benders decomposition [8], and branch and bound [9]. Inspired by these powerful approaches, in this work we extend the dimensionality reduction algorithm to nonlinear MaOPs using an outer approximation-like strategy. The remainder of this paper discusses this approach and is structured as follows. Next, the algorithm for systematically reducing dimensionality of nonlinear MaOPs is described in detail. We then introduce the DZLT5 suite of benchmark MaOP's and discuss why it is an ideal testbed for our algorithm. Then, we present the results of applying our algorithm, making note of the effects of key hyperparameters used in the algorithm. Finally, we provide some concluding remarks and open questions for future work.

METHODOLOGY

Nonlinear Dimensionality Reduction Approach

Consider a nonlinear MaOP (Multi-objective Optimization Problem) of the following general form:

$$\min_{x} \{f_1(x), \dots, f_r(x)\}$$
$$s.t. \quad g(x) \leq 0$$

In our previous work [5], we identified that projecting objective cost vectors onto constraint surfaces provided the necessary information for determining groups of correlated objectives. We take a similar approach here, systematically generating approximate linearized constraint surfaces using a first-order Taylor expansion around a feasible fixed point x^n ,as depicted in the equation (1). As additional fixed points are incorporated into the process, the resulting linear constraints progressively provide a closer approximation of the original nonlinear problem when the problem is convex.

$$g(x) \approx g(x^n) + \nabla g(x^n)(x - x^n) \tag{1}$$

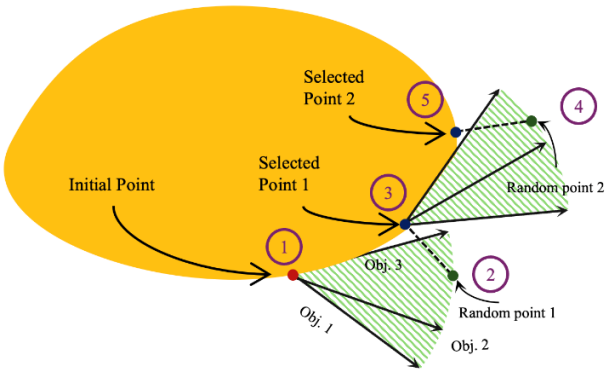

Figure 1: How the algorithm choose points. Numbers in the circle shows the sequences of the process.

However, one primary challenge must be addressed to effectively develop this nonlinear method. The challenge involves determining the optimal method for selecting the set of fixed points from which the relaxed linear constraints are derived. We propose a systematic approach that identifies fixed points along the projected gradient descent paths of the objectives. Figure 1 shows how we select the fixed points and the numbers in the purple circle indicated the sequence of the process. It starts from a (set of) initial point x^n on the boundary of g. Directions inside the cone of objective gradient vectors indicate directions from the fixed points where the tradeoffs are most likely to occur within this optimization problem, as moving in these directions will improve some objective values. Thus, by strategically selecting new fixed points within the cone of projected objective gradients, new linearized constraints are generated which tend to be concentrated in regions where objective conflicts are most pronounced, that is, along nonlinear

constraints which are active in determining the Pareto frontier.

Unlike linear optimization problems, nonlinear MaOPs can feature single-objective optimal solutions situated within the interior of the feasible region. Therefore, unlike in the linear case, it is crucial to consider the interactions of objectives along constraints where both objective gradients point into the feasible region, which were neglected previouslyWe define a new gradient operator $\nabla f_i(\cdot)_k^*$, which is equal to the projection of the gradient of objective i onto constraint k if the gradient vector points out of the feasible region, and simply equals the gradient of objective i if the gradient points into the feasible region. Then, for each pair of objectives i and j, the correlation strength along constraint k linearized at fixed point n, S_{ijkn}, is:

$$S_{ijkn} = \nabla f_i(x^n)_k^* \cdot \nabla f_j(x^n)_k^* \quad (2)$$

To fully detemine objective correlations, a systematic approach is required for generating new fixed points to use in the generation of linearized constraints. The process for doing so is as follows: first, a random step direction Δ is chosen that is a conic combination of all projected linearized objectives, such that:

$$\Delta = \frac{\sum_{i=1}^{I} \omega_i \nabla f_i(x^n)_k^p}{\sum_{i=1}^{I} \omega_i} \quad (3)$$

where ω_i are random values between 0 and 1. A user defined step size parameter α in equation (4) is used to make the fixed point selection more flexible. With this Δ , a new point (i.e. random point 1 in Figure 1) is obtained: $x^n + \alpha\Delta$. This point may not be feasible to the original problem, so a new feasible point is generated by projecting this point back to the feasible set denoted *X*.

$$x^{n+1} = \text{argmin}_{x \in X} |x - (x^n + \alpha\Delta)|_2^2 \quad (4)$$

In Figure 1, this generates selected fixed point 1 which is the nearest feasible point to the random point 1. This process is repeated applied to the selected fixed points to generate next ones as shown in step 4 and 5 in Figure 1. At each selected fixed point, constraints are linearized and objective correlation strengths are determined using eqn. (2).

Once a sufficient number of fixed points have been generated, we can compile all of the objective correlation strengths into a single value using the same approach as in the linear algorithm:

$$S_{ij}^A = 0.5\left(1 + \frac{\sum_{k=1}^{K}\sum_{n=1}^{N} W_{ijkn} S_{ijkn}}{\sum_{k=1}^{K}\sum_{n=1}^{N} W_{ijkn}}\right) \quad (5)$$

Here, W_{ijkn} is weight that is calculated based on the value of S_{ijkn}, taking into account that a competition along a single constraint can cause competition between objectives. We assume that the linearly relaxed constraint space sufficiently approximates the important parts true constraint space for determining objective correlation, enabling the generation of reasonable correlation strengthsThese strengths become the edge weights in an objective correlation graph, which is a fully connected graph where nodes correspond to objectives in the MaOP. Finally, community detection is used on this graph to identify objective groupings for dimensionality reduction.

The nonlinear objective reduction algorithm has two key hyperparameters: the first, as previously described, is the step size to use when generating new fixed points, while the second is the number of fixed points used to determine objective correlation. Determination of the appropriate values to use for each will be assessed using computational experiments that look at, for example, how much new information is added from one additional linearized constraint, and discussed in the results and discussion section.

DTLZ5(I, M) Problem Set

DTLZ5(I, M) provides MaOPs with a well-defined structure and known objective correlations. Problems from this test set can be of arbitrarily large objective dimensionality It has been widely used to test multi-objective evolutionary algorithms [10], the current state of the art for solving large scale MaOPs. In this problem set, *M* denotes the number of objectives and *I*<*M* denotes the true dimensionality of the Pareto frontier. All objectives are to be minimized.

$$\min_x \{f_1(x), \ldots, f_M(x)\}$$

$$f_1 = (1+g)\,0.5 \prod_{i=1}^{M-1} cos(\theta_i)$$

$$f_{m=2:M-1} = (1+g)\,0.5 \prod_{i=1}^{M-m} cos(\theta_i) sin(\theta_{M-m+1})$$

$$f_M = (1+g)\,0.5\, sin(\theta_1)$$

$$g = \sum_{i=M}^{M+k-1} (x_i - 0.5)^2$$

$$\theta_{i=1:I-1} = \frac{\pi}{2} x_i$$

$$\theta_{i=I:M-1} = \frac{\pi}{4(1+g)}(1+2gx_i)$$

$$0 \le x_i \le 1, for \ \ldots = 1,2,\ldots,n$$

$$n = M + k - 1$$

All objectives within {f1, . . . , fM−I+1} are positively correlated, while each objective in {fM−I+2, . . . , fM} is conflicting with every other objective in the problem.This

implies that the correct grouping of objectives is to group objectives {f1, . . . , fM−I+1} into a single group, while keeping all remaining I-1 objectives in their own groups. In this work, we choose k = 10, as is consistent with other works using this benchmark problem set. Additionally, the optimal points from the optimization results of individual obejctives of DTLZ5 are used as initial points.

RESULTS AND DISCUSSION

Our nonlinear dimensionality reduction method has been applied to the DTLZ5 problem set, beginning with DTLZ5(2,3) to assess the feasibility of our algorithm. Our algorithm effectively identified correlated objectives and correctly segmented the multi-objective optimization problem into [f1, f2] and [f3]. This categorization indicates that f1 and f2 are correlated, and both are in competition with f3. This outcome precisely aligns with the specifications defined in the DTLZ5(2,3) problem, confirming the accuracy of our approach.

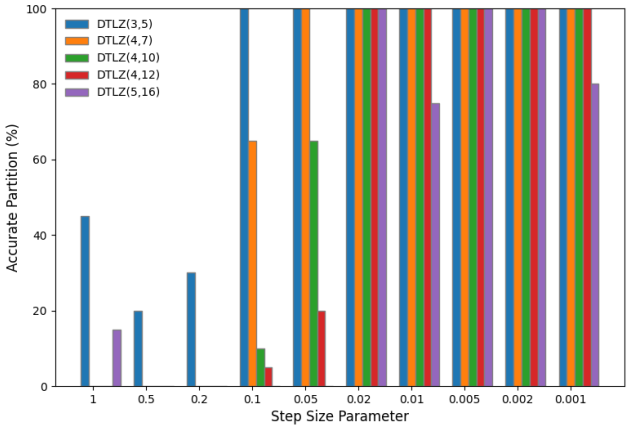

Figure 2: Accurate Partition vs Step Size Parameters in different DTLZ5 problems.

However, when testing larger problems such as DTLZ5(3,5) and DTLZ5(4,7), the results are sometimes accurate, but the overall accuracy seemingly decreases as the complexity of the problem increases. This issue may be influenced by the magnitude of the step size hyperparameter used to generate the next selected point. If the step size is too large, it can cause the selected point to fall outside of the region of the feasible space that is active in determining the Pareto frontier, reducing the utility of the linear constraints generated. This effect is consistently observed when selecting fixed points.

To address this, we conducted tests on step size parameters across different DTLZ5 problem sets, as shown in Figure 2. We varied step size parameters from 1 to 0.001 across DTLZ5(3, 5), DTLZ5(4, 7), DTLZ5(4, 10), DTLZ5(4, 12), and DTLZ5(5, 16), using 40 selected fixed points for each objective. Objective groupings for each problem were computed 20 times to mitigate the effects of randomness in step directions. The results show that our algorithm can achieve about 25% or higher accuracy in the DTLZ5(3, 5) tests, even with a large step size parameter. Interestingly, with a step size parameter of 1 in DTLZ5(2, 3), the algorithm still produced high accuracy results, suggesting a high probability of achieving correct results by chance without accurately capturing the conflict zone. When the step size parameter is reduced to 0.1 or lower, the algorithm consistently achieves 100% accuracy, indicating that a smaller step size enhances performance. This trend is also observed in DTLZ5(4, 7), DTLZ5(4, 10), and DTLZ5(4, 12), although the required step size for 100% accuracy decreases as the problem set complexity increases.

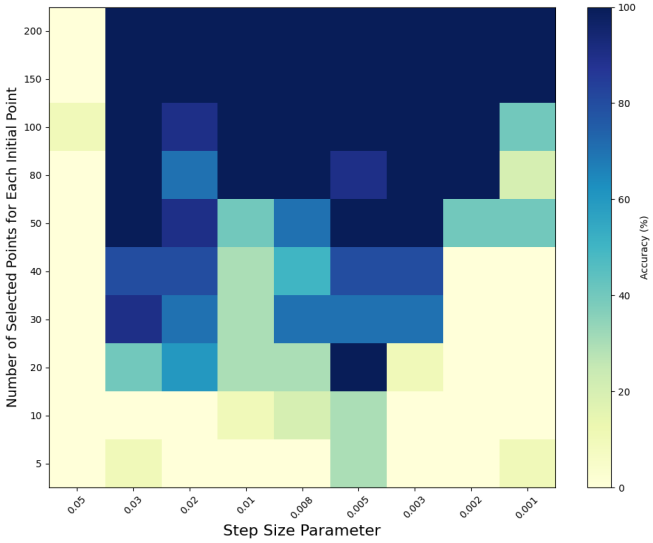

Figure 3: Heat map for accuracy of DTLZ(5,20) test results. Each grid in the graph is calculated 10 times with corresponding step size parameters and number of selected points for each starting points.

However, the tests for DTLZ5(5, 16) show relatively lower accuracy when the step size is very small. This suggests that the algorithm's performance can degrade with too small a step size. As the dimension increases, more fixed points are required to move to potential conflict areas. The average random step size direction Δ also increases with dimensionality. For instance, the average Euclidean distance of random step size direction is about 0.0166 in DTLZ5(3,5), increasing to about 0.0259 in DTLZ5(5,20) with the same step size parameter of 0.03. Therefore, for complex datasets like DTLZ5(5,20), a smaller step size and more selected fixed points are needed to ensure comprehensive mapping of the space and effective location of conflict areas.

To further illustrate the computational performance effected by step size parameter and the number of selected points, a heat map combined with different

selected points and step size parameters are shown in Figure 3. Step size parameter larger than 0.05 would never give a high accuracy results even when 200 selected points are chosen for computation. This matches the conclusion from Figure 2. In this problem set, each variable can feasibly vary between 0 and 1, while from Figure 3, accurate results begin to generate at 0.03. Thus, for this problem it seems a step size of about 3% of the range of the most flexible dimension of the feasible region should be sufficient for most cases in the DTLZ set; however, this finding may be problem-dependent. Moreover, increasing the number of selected points such that the product of the number of steps and step size exceeds the half of longest distances between all the initial points seems to yield good results. A tradeoff clearly emerges similar to that observed in gradient-based optimization: a smaller step size normally will generate higher quality results more reliably, but may require a larger number of iterations, and computational effort, to do so.

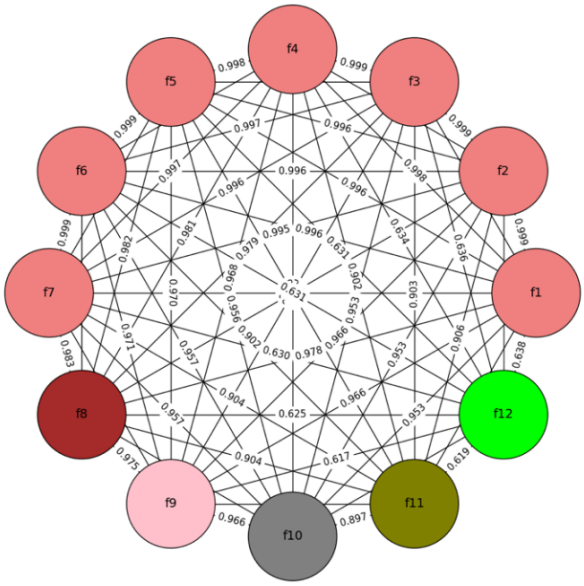

Figure 4: Graph results of DTLZ5(6,12). Nodes with the same color indicate that they are in the same group.

After tuning the step size parameter and the number of selected fixed points, the correlating and competing nature of objectives in DTLZ5(5,20) was successfully detected by our nonlinear algorithm. Due to visualization challenges, the graph results of DTLZ5(5,20) are not shown; instead, results from DTLZ5(6,12) are displayed in Figure 4. The lines between different nodes represent the edges indicating the correlation strength between different objectives. Clearly, the largest edge weights, corresponding to pairs of objectives most strongly correlated, occur connecting objectives 1-7, as would be expected for this problem instance.

The time cost of the algorithm for instances of different size was evaluated on a MacBook Air with an M1 CPU and 16GB RAM to assess the algorithm's scalability. In Figure 5, the blue segment illustrates the time spent generating selected points for different optimization problems, while the orange segment indicates the time taken to generate the graph and apply community detection. In this test, each problem includes a total of 240 selected fixed points. Fixed points are generated starting from the optimal solution for each individual objective, which accounts for the slight increase in fixed point generation time as a function of number of objectives. However, the majority of the increase in time as a function of objectives is attibuted to the time required to generate and detect structure in the objective correlation graph. This is consistent with the fact that the number of edge weights calculated is quadratic with the number of objectives, and the community detection algorithm also providing polynomial scaling with number of objectives (graph nodes).

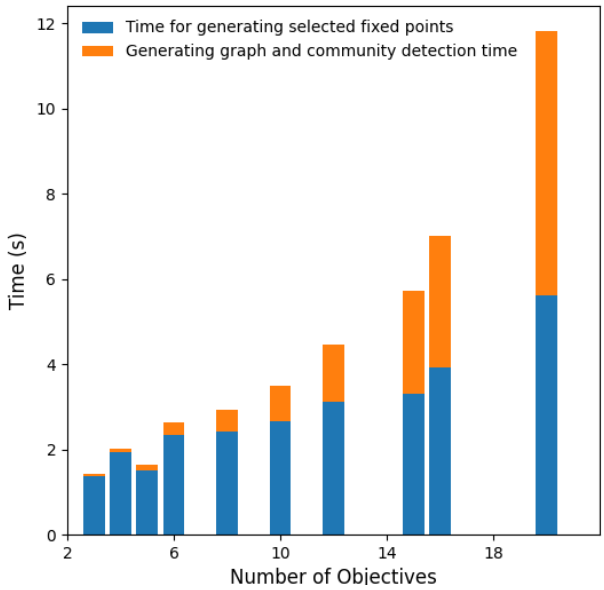

Figure 5: Bar graph for time usage of the algorithm with different number of objectives. Total selected points for each of the test is 240.

The relationship between calculation time and the number of selected points is illustrated in Figure 6. To mitigate fluctuations caused by randomness, each data point was calculated 20 times to ensure robustness. As evident, the calculation time increases linearly with the number of selected points, although the slopes vary across different datasets. This trend of increasing slopes corresponds with the observations in Figure 5. Furthermore, the consistent overlap of red and green dots indicates that variations in the step size do not significantly affect the calculation time.

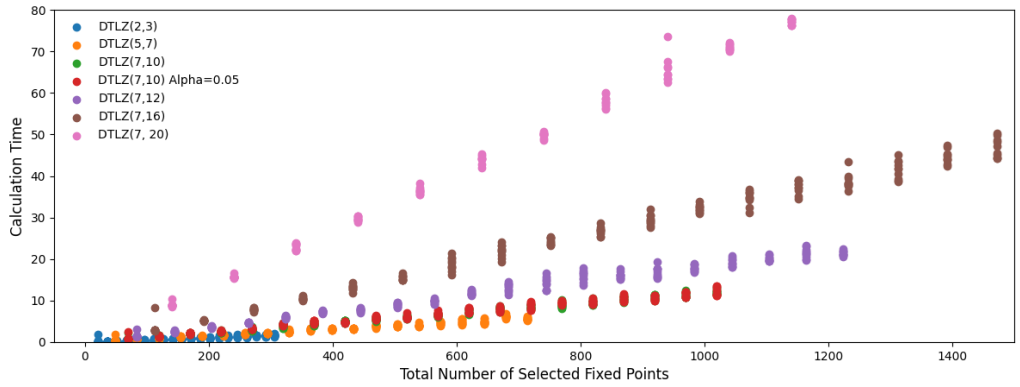

Figure 6: Calculation time versus number of selected fixed points in different DTLZ(I,M) problems. Step Size parameter is 0.03 without special annotation.

CONCLUSION

In this study, we build upon the many-objective dimensionality reduction algorithm developed by our group for linear problems, by introducing a novel algorithm that extends this approach to a nonlinear framework. Utilizing an outer approximation-like method, nonlinear objectives and constraints are converted into linear forms, which are then processed using our existing linear algorithm with minor modifications.

We tested our enhanced algorithm using the DTLZ5(I, M) problem set, a benchmark in many-objective optimization. By carefully adjusting hyperparameters, including the step size and the number of selected fixed points, our algorithm successfully identified the correlating and competing nature of the DTLZ5(I, 20) problem. Additionally, the performance and scalability of the algorithm in terms of computational time is also demonstrated, aligning well with our expectations based on the algorithm's structural design. In the future, we aim to apply this algorithm to problems of practical interest for sustainable decision making in the chemical process industry.

ACKNOWLEDGEMENTS

Financial support for this work was provided by the National Science Foundation (NSF) CAREER Award (CBET-2237284).

REFERENCES

1. Sahinidis NV. BARON: A general purpose global optimization software package. *Journal of global optimization*, 8, 201-5 (1996).
2. Wächter A, Biegler LT. On the implementation of an interior-point filter line-search algorithm for large-scale nonlinear programming. *Mathematical programming*, 106,25-57 (2006).
3. Rangaiah GP, editor. Multi-objective Optimization: Techniques and Applications in Chemical Engineering. world scientific (2016).
4. Wu Q, Liu X, Qin J, Zhou L, Mardani A, Deveci M. An integrated multi-criteria decision-making and multi-objective optimization model for socially responsible portfolio selection. *Technological Forecasting and Social Change*, 184, 121977 (2022)
5. Russell JM, Allman A. Sustainable decision making for chemical process systems via dimensionality reduction of many objective problems. *AIChE Journal*. 69(2), e17962 (2023).
6. Wang H, Allman A. Analysis of the correlating or competing nature of cost-driven and emissions-driven demand response. *Computers & Chemical Engineering*, 181, 108520 (2024).
7. Marco AD, Ignacio EG. An outer-approximation algorithm for a class of mixed-integer nonlinear programs. *Mathematical programming*, 36, 307–339 (1986).
8. Arthur MG. Generalized benders decomposition. *Journal of optimization theory and applications*, 10, 237–260 (1972).
9. Evelyn MLB. Branch and bound methods for mathematical programming systems. *In 17 Annals of Discrete Mathematics*, 5, 201–219 (1979).
10. Deb K, Thiele L, Laumanns M, Zitzler E. Scalable Multi-objective optimization test problems. *Proceedings of the 2002 Congress on Evolutionary Computation. CEC'02 (Cat. No. 02TH8600)*. 1, 825-830 (2002).